14TH CANADIAN MASONRY SYMPOSIUM
MONTREAL, CANADA
MAY 16TH – MAY 20TH, 2021

EVALUATION OF SECOND-ORDER EFFECTS IN SLENDER REINFORCED MASONRY WALLS

Bilotta Rios, Miguelangel[1] and Cruz Noguez, Carlos[2]

ABSTRACT

Masonry load bearing block walls represent the most frequently used structural components between different type of masonry systems for the construction of industrial buildings. Therefore, the development of a rationalized design procedure able to provide adequate axial capacity and bending stiffness to resist the effects of axial load and out of plane (OOP) bending is vital. The continued effort of many researchers has made possible the use of Reinforced Masonry Walls (RMWs) with increasingly higher slender ratios in current structures in Canada. Nevertheless, developing the ideal design procedure has been a challenging and endless task. To date, most design codes do not exhibit a consistent and effective approach to consider the secondary orders or (P-Δ) effect in Slender Masonry Walls (SMWs). The current Canadian standard (CSA S304-14) and the Building Code Requirements and Specification for Masonry Structures (TMS/402/602-16), used in United States, have adopted the Moment Magnifier (MM) method to quantify the P-Δ effect in the design of SMWs. The methodology intends to estimate an amplification factor that depends on the Euler Buckling Load based on the actual flexural stiffness of the MW. Although the same philosophy is followed by both committees, each standard has defined different mechanisms to obtain the parameters needed to apply the MM. A fibre finite element model has been validated on the basis of previous experimental test reports. The finite element results are compared with the current MM methods proposed by each standard and their effectiveness is evaluated. A new expression to quantify the OOP stiffness based on a regression analysis is proposed.

KEYWORDS: *reinforced masonry, slender wall, out-of-plane behaviour, moment magnifier, second-order effects, effective stiffness.*

[1] MSc student, University of Alberta, 116th St. & 85th Ave., Edmonton, AB, Canada, bilotta@ualberta.ca
[2]Associate Professor, Department of Civil and Environmental Engineering, University of Alberta, 116th St. & 85thAve., Edmonton, AB, Canada, cruznogu@ualberta.ca

INTRODUCTION

Masonry has proven to be one of the most durable and reliable construction materials since the beginning of civilization. Earliest masonry structures were usually excessively conservative, and many arbitrary restrictions were considered due to the limited knowledge available. In recent years few experimental and analytical research programs were conducted forming the bases of the Canadian Masonry Design Standard "Design of Masonry Structures" [1] and the "Building Code Requirements and Specification for Masonry Structures" [2], which is the American proposal. Nowadays, masonry structures are still widely used for residential and commercial purposes, offering an excellent alternative to other materials available in North America, such as steel, wood or concrete.

Developing rational design procedures has been an endless and challenging task, as many researchers have proven [3],[4]. During the design of slender masonry walls, special attention must be given to second-order effects [5]. Any attempt to predict the Out Of Plane (OOP) behaviour accurately in Reinforced Masonry Walls (RMWs) appears to be impossible if the material and geometrical nonlinearity are not considered. Hatzinikolas et al. [6] conducted an experimental program to study the geometrical nonlinearity with specimens, ranging in slenderness ratio from 13.8 to 24 and subjected to eccentric loading. The samples were tested using pinned-pinned boundary conditions. The study proposed a new method adopting the Moment Magnifier (MM) from reinforced concrete which utilized an Effective Rigidity (EI_{eff}) concept, which attempts to predict the flexural rigidity of masonry walls based on the estimated extent of cracking in the cross-section of the specimen. Although its longevity, the (EI_{eff}) concept is still used in the current Canadian standard. The American committee adopted a different alternative, accepting the MM procedure, while the flexural rigidity is calculated based on the cracked modulus of inertia ($E_m I_{cr}$). Both solutions (EI_{eff} and $E_m I_{cr}$) have proven to be conservative [7],[8] in predicting the flexural rigidity for some circumstances.

This paper presents a pilot study that evaluates the second-order effects on Reinforced Masonry Walls (RMWs) using a fibre-based finite element model. The numerical model was validated on the basis of previous experimental programs [9],[10]. Analytical moment amplification factors are calculated and compared against those computed using the CSA S304-14 and TMS 402-16. A new expression to estimate the flexural stiffness of fully-grouted walls is proposed. This equation was developed using a multilinear regression analysis with a total of 1381 data points.

FINITE ELEMENT EVALUATION

A fibre-based model was created using the Open System for Earthquake Engineering Simulation (OpenSees) to evaluate the OOP behaviour of fully-grouted RMWs subjected to concentrically and uniformly distributed lateral pressure [11]. OpenSees is an object-oriented software framework for simulations application using finite element methods able to predict accurately the response of highly nonlinear systems. The OOP behaviour of the wallets was simulated using a NonLinearBeamColumn element available in the OpenSees library. The element uses a force-

based formulation able to capture material nonlinearity through the spread of plasticity along the fibre-section. Geometrical nonlinearity was considered by implementing a *Corotational* geometric transformation law. The boundary conditions were set up as pinned-pinned for all the simulations ($k = 1$).

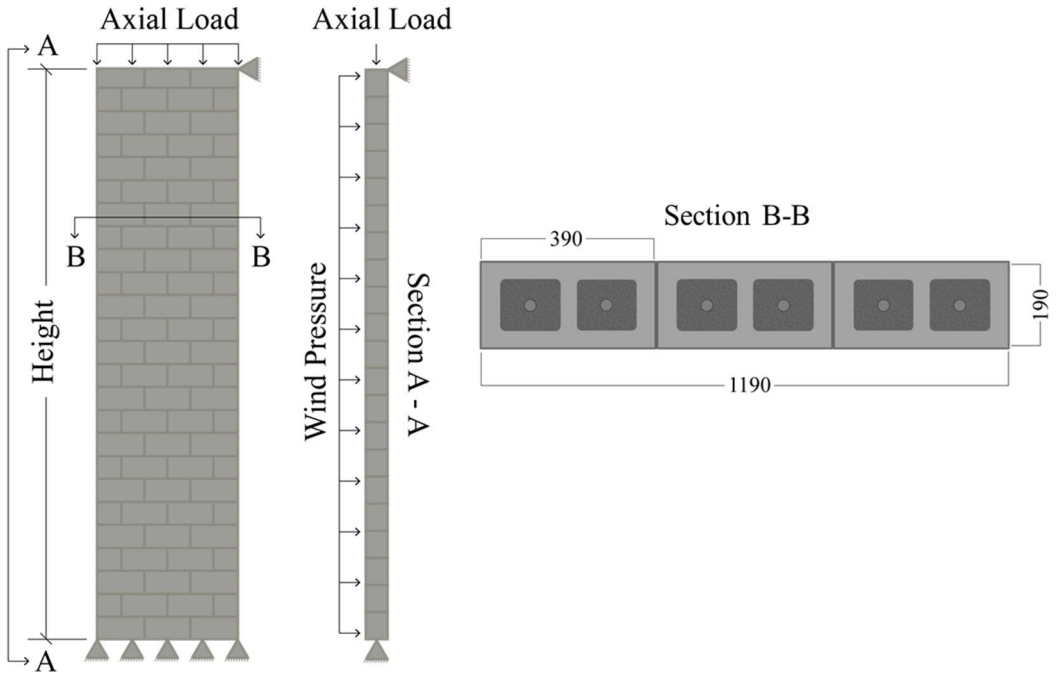

Figure 1: Masonry wall section. Units in mm.

Material Properties

The homogenous behaviour of the masonry was simulated using *Concrete02*, a uniaxial stress-strain law from the OpenSees library based on the Kent-Scott-Park model [12]. A parabolic stress-strain relationship is assumed up to the maximum compressive stress of the masonry, followed by a linear softening branch stopping at the maximum crushing strain. The material also assumes a linearly tensile strength increment, which is followed by a linear tension softening branch to failure

The model proposed by Priestley and Elder [13] to evaluate the homogenous behaviour of the masonry assemblage was adopted in this study to calculate the ultimate and crushing stress of the masonry fibres; the maximum compressive strength is assumed to happen at a strain of 0.002. Priestley and Elder's model demonstrated excellent results on partially grouted specimens. The material model also presents a perfect correlation with the "Concrete02" parabolic stress-strain distribution. The longitudinal steel reinforcement was simulated using the uniaxial material model "*Steel02"* with isotropic strain hardening based on the Giuffre-Menegotto-Pinto [14] model. Figure 2 shows the constitutive relationship implemented in the FEA model.

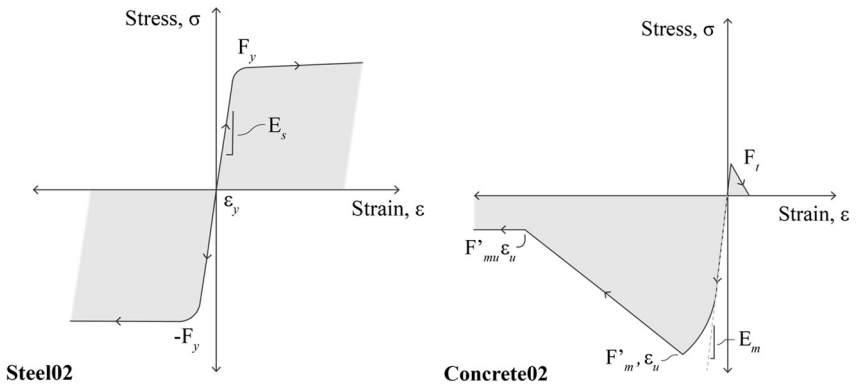

Figure 1: Material Constitutive Relationships. Steel (left) and Masonry (right)[Adapted from Priestley and Elder]

Model Validation

To determine the performance of the model, two experimental programs with different loading scenarios were used. The first campaign corresponds to the experimental results of slender masonry walls from the ACI-SEASC Task Committee on Slender Walls (Figure 3a), which have formed the basics of current design standards in Canada and United States, and although its longevity is still one of the most comprehensive programs to validate any Finite Element (FE) model of RMWs. Moreover, to evaluate partially-grouted specimens, the experimental program conducted by Mohsin in 2003 at the University of Alberta was selected (Figure 3b).

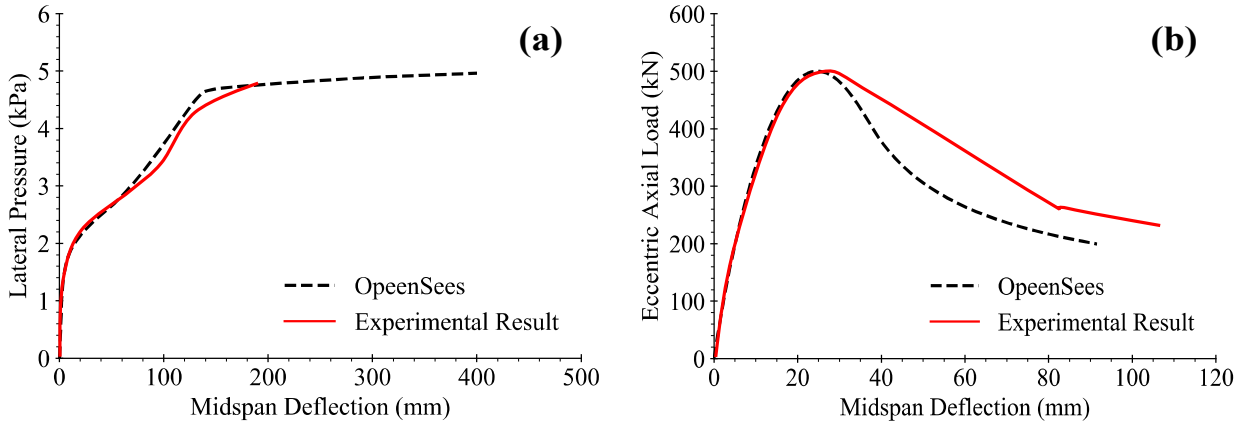

Figure 3: Finite Element Model validation. (a) SEAC Panel [10] (b) Mohsin W8 [9].

NUMERICAL RESULTS

The moment amplification factors obtained as per the Canadian standard and the American standard are compared against those from the analysis model for different values of axial load, slenderness ratio, and compressive strength per each reinforcement ratio. The amplification factors were calculated using the moment magnifier method.

Multiple simulations were held, but only fully-grouted walls were studied. A constant cross-section geometry was used for all the analyses (Figure 1). The variation of axial loading, slenderness ratio, reinforcement ratio and masonry compressive strength in the flexural stiffness was explored. Table 1 illustrates the parameters and the variation rate used per each simulation. The selection of the axial loading range was consulted with Canadian designers. Multiple slenderness level was selected to compare the evolution of the second-order effects as the slenderness ratio increases. With a constant block thickness throughout the simulations (190 mm), the wall height was increased by 2m per each step. The maximum height is 12m (h/t = 60), which represents a very slender wall that is not typically constructed in North America. The minimum reinforcement ratio, ρ, selected for the analysis (0.5) is equivalent to six rebars with the least steel area available in Canada (10M). The maximum ρ represents a highly reinforced structure with six 25M bars. The typical yield strength of the reinforcement ratio in Canada and the United States was used (400 MPa). Three levels of compressive strength of the masonry were adopted. Low (10 MPa), medium (20 MPa) and high compressive strength levels (30 MPa).

A total of 1575 simulations were held. The axial loading were applied using a load-control protocol. Once the specified axial load was reached, the lateral pressure was applied step by step using a displacement control protocol until the ultimate lateral load is reached or a maximum compressive strain of the masonry of 0.003 was reached. Any simulation that does not reach the specified maximum crushing strain of the masonry due to convergency issues was not considered in the analysis unless the ultimate lateral load was achieved before the analysis stopped. The amplification factors were calculated at ultimate load.

Table 1: Numerical Evaluation Matrix

Parameter	Range	Variation per simulation	Total Variations
Axial load (kN/m)	5-105	5 kN/m	21
Slenderness ratio (h/t)	20-60	10	5
Steel reinforcement ratio ρ (%)	0.5 – 2.5	0.5	5
f'_m (MPa)	10-30	10	3
f_y (MPa)	400	-	-
Steel Modulus of Elasticity (GPa)	200	-	-
Block Thickness (mm)	200	-	-

Figure 4 shows the ratio of M1/Mt versus the axial load for a reinforcement ratio of 1.0 calculated as per CSA S304-14 and TMS 402-16. This study only presents the results of reinforcement ratio of 1.0. M1 in the graph refers to the max applied moment caused by the lateral pressure, while Mt is the total moment, which includes the primary and second-order moments. M1/Mt refers then to the inverse of the moment magnification factor. The moment magnification factor is the factor the primary moment must be multiplied by to obtain the moment capacity or design moment of the

wall. The smaller the ratio M1/Mt is, the bigger the second-order effects are. The CSA S304-14 expression neglecting the reduction factor φ_e is also included to evaluate the consequences of reducing by 25% the cracked moment of inertia. It is important to consider throughout the discussion that the relative differences in the amplification factors presented might not only be attributed to the inability to calculate the stiffness of walls accurately using the expression proposed by the North-American standards. In an attempt to evaluate the efficacy of the MM method, amplification factors computed with an analytical effective stiffness ($E_m I_{eff}(M/\emptyset)$) are also presented. The rigidity was calculated using the principles of the euler bernoulli beam theory, where the division of the moment over its curvature represents the flexural rigidity. The curvature was calculated from the strain profiles by dividing the masonry strain at ultimate load by the depth of the neutral axis $\phi = \frac{\varepsilon_m}{c}$.

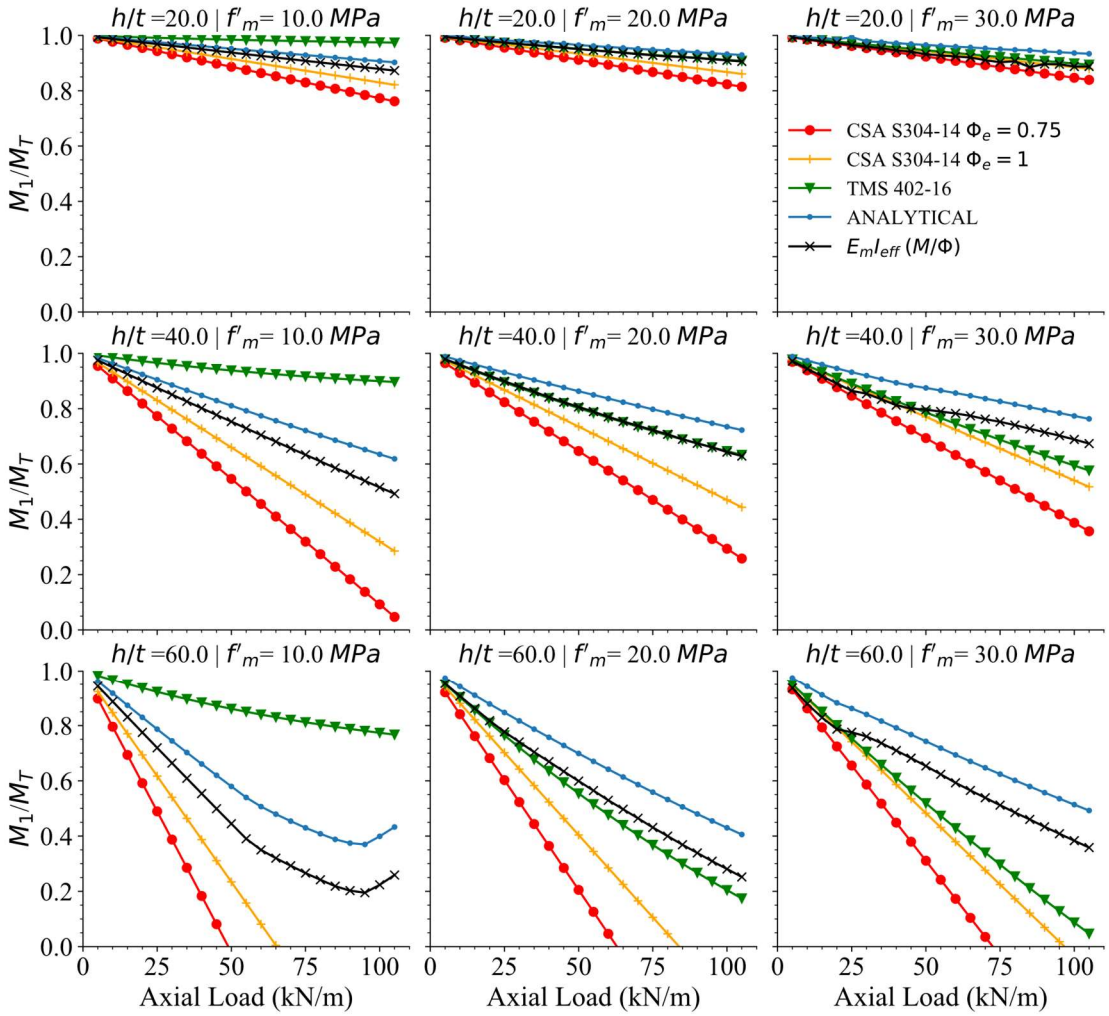

Figure 4: Comparison of Second-Order Effects from Analytical model to North-American standards (M1/MT). For ρ = 1.0

The sudden changes of the M1/Mt values in Fig. 4 are due to second-order effects, which from that point onwards, predominate greatly and ultimately reduced the total moment reached at ultimate load. This indicates that instability effects are so predominant that possibly walls designed under that parameters are not feasible for its construction.

The Canadian expression is the most conservative in all the scenarios. Gradual increment in the axial loading leads to an exponential rise in the percentage of error of the magnification effects compared to the numerical model results. The moment magnification factor relies on the ratio between the applied axial load and the, $P_{cr,}$ (P/P_{cr}). The expression proposed by CSA does not exhibit the influence of the axial loading in the calculation of the effective stiffness; consequently, the P_{cr} is only dependant on the mechanical properties of the cross-section, such as the amount of steel and the compressive strength (f'_m). While the axial loading is making the walls stiffer in the numerical model, the P_{cr} proposed by the Canadian expression remains constant. Under middle levels of slenderness ratio and compressive axial forces, the percentage of error range between 100% and 800%, which is equivalent to amplifying the primary moment 2 times and 16 higher than required. For High axial load levels, the approach is not only ineffective but inapplicable. The applying load exceed the P_{cr} calculated even at $h/t = 30,$ while the numerical analysis only showed instability issues for walls with ratios greater than 40. Consequently, an amplification factor cannot be calculated in many circumstances where the failure mode is not dominated by instability. Penalizing the flexural stiffness by a reduction factor $\emptyset_e$ seems unnecessary. Although the factor intends to predict any uncertainties, the degree of conservatism is so high that the factor becomes unnecessary. The equation's performance improved considerably when the factor is removed, mainly for short walls under low axial load. Nevertheless, as the slenderness ratio increases, the moment amplification still extremely conservative and unviable.

The amplification effects according to the TMS 402-16 demonstrate to produce generally conservative results. For the steel ratio presented in Figure 4, the moment amplifications becomes greatly unconservative whenever 10 MPa (f'_m) is used. To some extend, the cracked moment of inertia calculated exceed the gross inertia, which is physically impossible. The same phenomenon occurs for reinforcement ratio of 2 and 2.5, using a masonry compressive strength of 20 MPa (not presented in this study). Analyzing the data reveals that the results calculated using the expression suggested by the American committee for the depth of the compressive masonry block, c, is incredibly higher compared to the depth obtained using the strain profiles from the numerical analysis, whenever 10 MPa is used. As the equation to calculate the neutral axis depth is developed empirically, it is possible that data points with $f'_m$of 10MPa was not available for its development. One particular virtue of the American approach is the fact that it considers a non-linear stress distribution and the interaction of the axial load in the flexural stiffness. Thus, the percentage of error is much lower compared to the CSA S304-14, particularly at high compressive forces levels. However, the calculations reveal up to 300% of error for very slender walls. Overall, the TMS 402-16 expression seems to be a viable solution for compressive strength levels greater than 10

MPa, and up to a slenderness ratio of 40. The P_{cr} was only exceed in few cases before the numerical model showed sudden changes due to instability effects.

Moment amplification factors calculated using the analytical effective stiffness seem to estimate second-order effects with a remarkable accuracy for reinforcement ratios of 1.0. As the axial loading and the slenderness kept increasing, the analytical flexural stiffness outperforms the CSA S304-14 and the TMS 402-16. The highest percentage of error achieved using the analytical stiffness is approximately 40%.

REGRESSION ANALYSIS

This section presents an equation (Equation 1) to calculate the effective stiffness of RMWS develop through a regression analysis, using the data points of the analytical flexural stiffness obtained from the strain readings in the section above. Although the M1/Mt ratio for a reinforcement ratio of 1.0 was only presented in this study, the set of data points described in Table 1 was used. The regression analysis was conducted using the *Sklearn* library available in the computer language Python. The performance of the proposed equation is graphically shown in Figure 5. Each point represents a wall from the data set develops using the numerical analysis. The red line is the ideal scenario, where the predicted stiffness is equal to the analytical stiffness. Both the training and the testing data are plotted. Any point above the red line overestimates the effective stiffness, while points below this line are conservative results. The closer the points to the red line, the better is the performance of the model. As for performance indicators, the Root Mean Square (RMSE) were selected as a measure of precision and the Mean Error (ME) as a measure of bias, while the $E_m I_{eff\ (predicted)}/E_m I_{eff\ (analytical)}$ ratios as a measure of accuracy. Data points of walls where instability effects cause a sudden change in the ultimate load are discarded. This would falsely indicate an enhancement of the flexural rigidity for structures in which failure mode is highly dominated by instability. The total data points considered for the regression analysis was 1381. The training data was set to 30% of the total number of walls.

$$
\begin{aligned}
&For\ \rho < 1.5 \\
&E_m I_{eff} = 6.021x10^6\, P + 5.92x10^5\, As + 1.075x10^7\, f'_m + 1.0632x10^7 \left(\frac{h}{t}\right) - 4.75x10^8 \\
&For\ \rho \geq 1.5 \\
&E_m I_{eff} = 2.07x10^6\, P + 5.77x10^5\, As + 5.052x10^7\, f'_m + 2.157x10^7 \left(\frac{h}{t}\right) - 6.602x10^8
\end{aligned}
\qquad (1)
$$

Where P is the axial load in kN, As represents the total areal of steel in mm^2, f'_m is the grouted compressive prism strength in MPa, and h/t is the height-thickness ratio. $E_m I_{eff}$ is expressed in $kN - mm^2$.

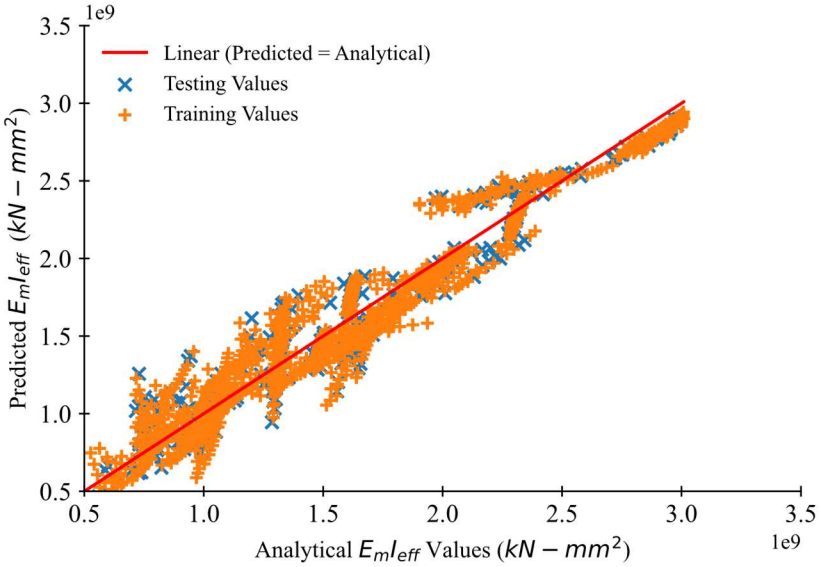

Figure 5: Regression plot MLR1

Performance indicators of the same data set used in the regression analysis are provided for the North American Standards equations in Table 2. MLR1 represents the expression developed in this study (Equation 1). Indicators for the Canadian expression assuming a reduction factor, $\emptyset_e$, equal to 1 are also included. Additionally, the performances of the American procedure were calculated for the entire data set and a filtered version. The filter version corresponds to data points with compressive strength values of 20 and 30 MPa. As discussed in the previous section, cracked moments of inertia computed using 10 MPa of compressive strength following the TMS procedure exceeded the gross inertia of the cross-section.

Table 2: Performance indicator comparison

Equation	R^2	**RMSE** $(kN - m^2)$	**ME** $(kN - m^2)$	$\frac{E_m I_{eff_{analytical}}}{E_m I_{eff_{predicted}}}$	
				Average	**Std. Dev**
MLR1*	0.93	155935	-1541	1.018	0.13
CSA S304-14 $\emptyset_e = 0.75$	0.84	819372	725337	0.574	0.352
CSA S304-14 $\emptyset_e = 1$	0.84	534896	435007	0.766	0.26
TMS 402-16	0.001	7628037	-3205211	3.04	0.43
TMS 402-16 (Filtered)	0.81	348424	17195	1.016	0.25

*Equation developed in this study

Of the existing equation, the Canadian expression had the best performance on the data. Although the expression improved considerably when the reduction factor $\emptyset_e$ is neglected, the indicators suggested an unacceptable performance. The average $E_m I_{eff}(analytical)/E_m I_{eff}(predicted)$ is close

to 0.5, indicating a high bias. Extremely high values of RMSE and ME also reflect high bias and variance. The American equation was the worst within the group. An average $E_m I_{eff}(analytical)/E_m I_{eff}(predicted)$ of 3.04 not only indicate deficient accuracy but also that the values are overestimated dramatically. If the data to evaluate the TMS 402-16 expression is filtered, and the calculations with a compressive strength of 10 MPa are not considered, the equation becomes the best solution from the existing equations. The average $E_m I_{eff}(analytical)/E_m I_{eff}(predicted)$ is very close to 1 and with a relatively low standard deviation, indicating low bias and a small spread of the calculated value. Nevertheless, using a filtered data set impedes a direct comparison. The equation generated in this study (MLR1) vastly outperform the existing expression, as indicated by the low error values and low standard deviation of the $E_m I_{eff}(analytical)/E_m I_{eff}(predicted)$ ratio. The RMSE from the MLR1 is approximately 3.5 times lower than CSA S304-14 equation and 2.23 lower than the TMS 402-16 equation with the filtered data. The ME is substantially smaller than any other alternative. Undoubtedly, all the indicators demonstrate that the proposed equation MLR1 is an effective solution under the data set on which it was developed.

CONCLUSION

This paper presents the results of a numerical program developed to assess the current method described in North American standards to compute second-order effects in RMWs. Additionally, an equation based on a multilinear regression analysis is proposed to calculate the effective stiffness of RMWs. From the numerical simulations, it was demonstrated that second-order effects calculated using the CSA S304-14 are very conservative. Even for 50 kN/m of axial loading and $h/t = 20$, the amplification factors double those produced by the fibre-based model. For higher axial loading and slenderness ratio, the percentage of error exceeded 800%. After a slenderness ratio of 40, axial loading higher than 50 kN/m exceeded the P_{cr} calculated using the CSA S304-14 equation. The reduction factor $\emptyset_e$ demonstrated to be unnecessary, as in most of the circumstances, the stiffness was underestimated. Second-order effects calculated following the TMS 402-16 provisions showed an acceptable percentage of error up to a slenderness ratio of 40 with f'_m higher than 10 MPa. For higher slenderness ratios, the percentage of error grew gradually. For compressive strength levels of 10 MPa the moment amplification factors were overestimated. Only in a few cases the P_{cr} was exceeded before the numerical model demonstrated pronounce instability effects. The moment magnifier method has proven to be a viable alternative to estimate the second-order effects for RMWs subjected to concentric axial loading and OOP bending under pinned-pinned conditions. If the analytical Effective Stiffness is used, the highest percentage of error reached was approximately 40%.

Based on the performance indicators, the proposed equation MLR1 vastly outperforms the current alternatives to estimate the effective stiffness of reinforced masonry walls under the parameters on which it was developed. Further research should focus on creating a more complete data set of numerical evaluations. A bigger data set would not only be beneficial to understand the flexural behaviour of RMWs under a wider range of parameters, but it will also provide more data points for further regression analyses.

ACKNOWLEDGEMENTS

The authors gratefully acknowledge the financial support of The Masonry Contractors Association of Alberta (MCAA), the Canadian Masonry Design Centre (CMDC) and the Alberta Masonry Council (AMC)

REFERENCES

[1] Canadian Standards Association (2014). "Design of Masonry Structures." *CSA S304-14.* Rexdale, ON, Canada

[2] The Masonry Society (2016). TMS 402/602. "Building Code Requirements and Specifications for Masonry Structures", *The Masonry Society (TMS),* Longmont, Colorado, USA.

[3] Cranston, W. B., and Roberts, J. J. (1976). "Structural Behaviour of Concrete Masonry - Reinforced and Unreinforced." *Structural Engineer*, 54(11), 423–436.

[4] Drysdale, Robert G. and Hamid, Ahmad A. (1983). "Capacity of Concrete Block Masonry Prisms Under Eccentric Compressive Loading." *ACI Journal.*, 102-108

[5] Pettit, C. (2019). *Effect of Rotational Base Stiffness on the Behaviour of Loadbearing Masonry Walls,* University of Alberta, Edmonton, AB, Canada.

[6] Hatzinikolas, M., Longworth, J., and Warwaruk, J. (1978b). Experimental Data for Concrete Masonry Walls*. University of Alberta - Structural Engineering Report No. 71*.

[7] Donà, M., Tecchio, G., & da Porto, F. (2018). "Verification of second-order effects in slender reinforced masonry walls". *Materials and Structures,* 51(3), 69.

[8] Liu, Y., and Dawe, J. L. (2003). "Analytical modelling of masonry loadbearing walls." *Canadian Journal of Civil Engineering*, 30(5), 795–806.

[9] Mohsin, E. (2005). *Support Stiffness Effect on Tall Load Bearing Masonry Walls*, University of Alberta, Edmonton, AB, Canada.

[10] ACI-SEASC Task Committee on Slender Walls, "Test Report on Slender Walls," American Concrete Institute and the Structural Engineers Association of Southern California, February 1980-September 1982, Los Angeles.

[11] McKenna, F. Fenves, G. Scott, H. Jeremic, B. (2000). "Open system for earthquake engineering simulation (OpenSees) [computer software]. Pacific Earthquake Engineering Research Center, University of California at Berkeley, California, USA.

[12] Kent, D. C., and Park, R. (1971), "Flexural members with confined concrete", *J. Struct. Div., ASCE*, 97(7), pp. 1969-1990.

[13] Priestley, M. J. N., and Elder, D. M. 1983. ''Stress–strain curves for unconfined and confined concrete masonry.'' *ACI J., 80-3*, 192–201

[14] Filippou, F. C., Popov, E. P., Bertero, V. V. (1983). "Effects of Bond Deterioration on Hysteretic Behavior of Reinforced Concrete Joints". *Report EERC 83-19*, Earthquake Engineering Research Center, University of California, Berkeley.